

STRUCTURE-BASED DESIGN OF COX-2 SELECTIVITY INTO FLURBIPROFEN

Christopher I. Bayly,* W. Cameron Black, Serge Léger, Nathalie Ouimet, Marc Ouellet, and M. David Percival

Merck Frosst Canada Inc., P.O. Box 1005, Pointe-Claire - Dorval, Quebec, Canada H9R 4P8

Received 11 November 1998; accepted 27 November 1998

Abstract: Comparative computer modeling of the X-ray crystal structures of cyclooxygenase isoforms COX-1 and COX-2 has led to the design of COX-2 selectivity into the nonselective inhibitor flurbiprofen. The COX-2 modeling was based on a postulated binding mode for flurbiprofen and took advantage of a small alcove in the COX-2 active site created by different positions of the Leu384 sidechain between COX-1 and COX-2. The design hypothesis was tested by synthesis and biological assay of a series of flurbiprofen analogs, culminating in the discovery of several inhibitors having up to 78-fold selectivity for COX-2 over COX-1. © 1999 Elsevier Science Ltd. All rights reserved.

Introduction: Cyclooxygenase (COX), also known as prostaglandin H synthase, is an enzyme implicated in the mediation of pain, fever, and inflammation. It catalyzes the oxidative conversion of arachidonic acid into prostaglandin H₂, a key intermediate in the biosynthetic pathway of prostaglandins, prostacyclins, and thromboxanes, which in turn mediate a variety of physiological effects both beneficial and pathological.¹ Recently it was discovered that two COX isoforms exist: COX-1, expressed constitutively in many tissues, and COX-2, an induced isoform having elevated expression in inflamed tissues. COX-1 is thought to be involved in ongoing "housekeeping" functions, for example gastric cytoprotection, while COX-2 is the isoform implicated in the pathological effects mentioned above.² Current COX inhibitors such as aspirin, ibuprofen, and indomethacin, used as nonsteroidal antiinflammatory drugs (NSAIDs), inhibit both COX-1 and COX-2 and have associated side effects of gastrotoxicity such as ulcer formation.¹ Thus there has been great interest in developing a COX-2 selective inhibitor to act as an effective NSAID without gastrotoxic side effects. The first published COX X-ray crystal structure was of sheep COX-1 complexed with flurbiprofen, a nonselective NSAID.³ Subsequently, the crystal structure of human COX-2 complexed with an indomethacin analog has been solved in these laboratories⁴ and other COX-2 crystal structures have also been determined elsewhere.^{5,6} Here we report our efforts to use the sheep COX-1 crystal structure and our human COX-2 crystal structure to rationally design COX-2 selectivity into flurbiprofen analogs.

Results and Discussion: Flurbiprofen (1) was modeled into the human COX-2 crystal structure⁴ and predicted to bind to COX-2 in a manner similar to COX-1,³ consistent with its nonselective behavior; this was used as the starting point for structure-based inhibitor design. Comparison of the crystal structures showed a potentially useful difference between the two isoforms in the upper part of the active site. A conserved residue, Leu384, is oriented differently in each isoform due to a sequence difference of neighboring residue 503. In COX-1, residue 503 is a phenylalanine whose large size pushes the Leu384 sidechain into the upper part of the active site (Figure 1a). In COX-2, the smaller Leu503 allows the Leu384 sidechain to orient itself towards the protein

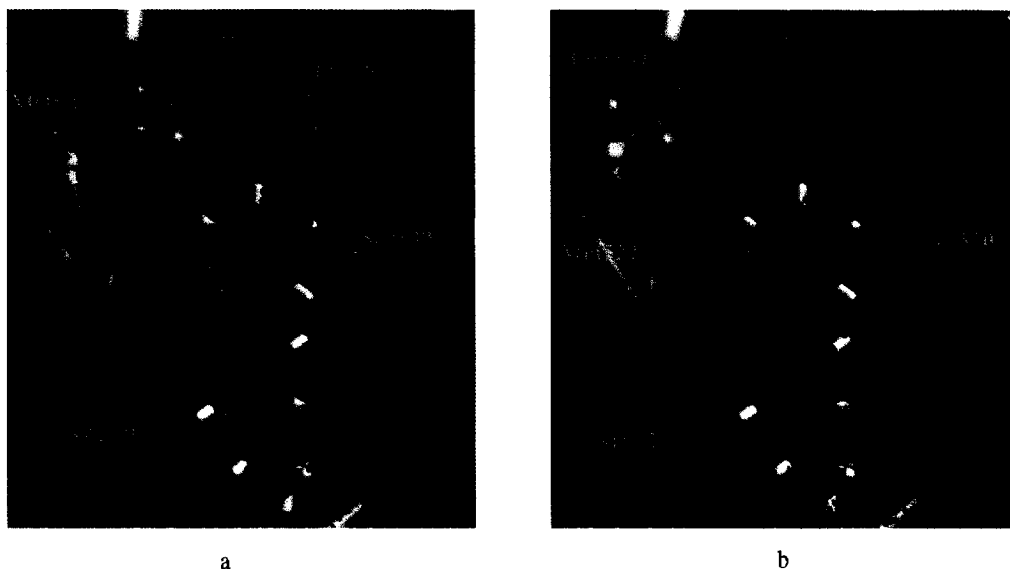


Figure 1. The cyclooxygenase active site (gray pipe backbone) and its molecular surface (blue dots) together with flurbiprofen **1** (with green carbons) docked in is shown for (a) COX-1 and (b) COX-2. In a, the Leu384 sidechain (gold) is pushed into the active site by Phe503 (not shown), leaving little space for a 3' substituent on ring A of flurbiprofen. In b, the Leu384 sidechain (gold) can adopt an orientation away from the active site, leaving a small alcove with enough room for a 3-atom 3' substituent planar with ring A of flurbiprofen. The alcove is additionally bounded by Tyr385 and Met522 in the plane of the figure, and by Trp387 in front and Phe381 behind the plane (not shown).

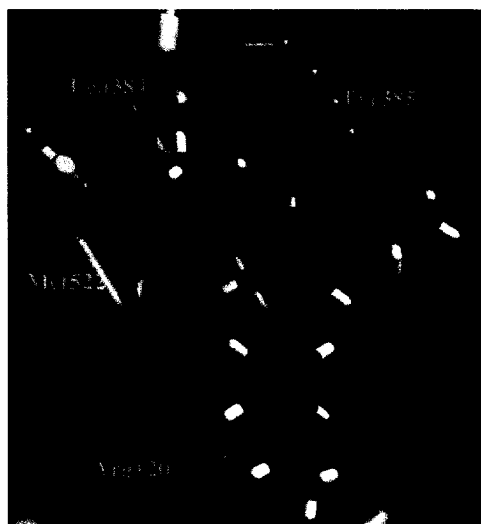
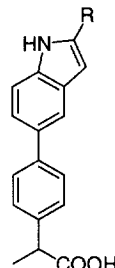
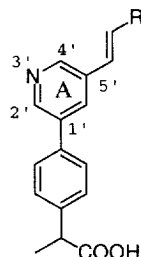
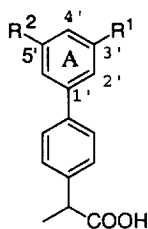
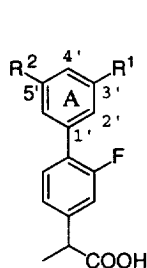


Figure 2. The minimized structure of the 3',5'-bisethoxy analog **8** complex with COX-2 after MD equilibration at 300K.¹¹ One ethoxy substituent occupies the Leu384 alcove and is responsible for the COX-2 selective behaviour, the other lies in the side channel and accepts a hydrogen bond from Tyr385. This binding mode is similarly implied for **4**. The nonselective monosubstituted 3' ethoxy analog **2** is proposed to owe its potency in COX-1 to placing the single ethoxy substituent in the side channel, which is similar in both enzyme isoforms.

away from the active site (Figure 1b). As a result, the COX-2 active site has more space in this region in the form of a small lipophilic alcove. An inhibitor placing a lipophilic group here could be expected to bind better to COX-2 than COX-1 because the inwardly-pointing Leu384 sidechain in COX-1 would cause an unfavorable steric interaction. As shown in Figure 1b, this alcove is located proximal to the 3' position of the ring A of flurbiprofen, leading to the design hypothesis that appropriate substitution of this position would introduce COX-2 selectivity. The orientation of the COX-2 alcove suggested that the substituent would need to be approximately planar with respect to ring A, and the limited size of the alcove would allow for only a relatively small substituent.

Initial testing of the hypothesis was done by the synthesis and assaying of the two 3' substituted flurbiprofen analogs **2** and **3**. The *in vitro* purified enzyme assay results are given in Table 1; for comparison purposes regarding COX-2 selectivity, IC₅₀s are also given for the two well-known COX-2 selective inhibitors DuP-6977 and NS-398.⁸ The ethoxy substituent of **2** was predicted to introduce COX-2 selectivity by occupying the alcove, and **3** was intended to test the ability of the inhibitor to shift in the active site in response to the steric interaction caused by the branching of the isopropyl substituent, which was too short to probe the depth of the pocket. Compound **3** showed a pronounced loss of activity compared to flurbiprofen, suggesting that the binding mode is not very flexible, an advantage for the design hypothesis. In contrast, the ethoxy analog **2** was of comparable activity to the parent compound, but surprisingly showed no COX-2 selectivity whatsoever. To understand the activity of **2**, re-examination of the crystal structures led to the rationalization that only a small shift of either the inhibitor or Tyr385 would be required to make a small side channel,⁴ which opens between Tyr385 and Ser530 and is similar in both isoforms (Figure 1), available to a ring A 3' substituent, given a 180° rotation of ring A. Furthermore, the ether oxygen of the substituent would be ideally placed to hydrogen bond with the hydroxyls of Tyr385 and Ser530. In COX-2 this would simply be another possible binding mode, but in COX-1 it would allow an energetically favorable alternative to the steric interaction implied by the design hypothesis. As a corollary, this rationalization also suggested that the desired COX-2 selectivity would be obtained by modifying the 3'-ethoxy analog **3** to the 3',5'-bisethoxy analog **4**, allowing one ethoxy substituent to occupy the side channel but forcing the other into the alcove location present only in COX-2. The subsequent synthesis and assay of **4** showed it to be a potent inhibitor of COX-2, albeit tenfold less than the parent compound, but exhibiting a 77-fold selectivity for COX-2 over COX-1. A more detailed kinetic analysis further showed that **4** was a time-dependent inhibitor of COX-2 but, unlike the nonselective flurbiprofen, was time-independent against COX-1. This different kinetic behavior of COX-1 and COX-2 is shared by other classes of COX-2 selective inhibitors^{9,10} including DuP-697 and NS-398. The 3',5'-bismethoxy analog **5** was active but nonselective, showing that the COX-1 active site still has enough room on the "alcove" side to accommodate a planar two-atom substituent. In contrast, the comparatively weak inhibition of the smaller 3',5'-bismethyl analog **6** may be due to the need for a good hydrogen-bonding substituent in the entrance to the side channel. To test the limits of the design hypothesis, further analogs were made in the more synthetically accessible des-fluoro series having parent compound **7**; assay results are given in Table 1. The 3',5'-bisethoxy analog **8** showed comparable potency and COX-2 selectivity to **4**. A snapshot of a molecular dynamics simulation¹¹ of **8** in COX-2 (Figure 2) shows how the two ethoxy substituents might occupy both the alcove and the side channel as proposed for the fluorinated analog **4**. Replacing the ether oxygen in **2** with sulfur to give **9** yielded a ninefold selective compound, showing that 3' monosubstitution of ring A alone could confer COX-2 selectivity, consistent with the original hypothesis. The much lower COX-1 potency of **9** compared to **2** suggests that the thioethyl group does not lie in the side channel as favorably as the ethoxy substituent.



- 1 $R^1 = H$, $R^2 = H$
 2 $R^1 = OEt$, $R^2 = H$
 3 $R^1 = iPr$, $R^2 = H$
 4 $R^1 = OEt$, $R^2 = OEt$
 5 $R^1 = OMe$, $R^2 = OMe$
 6 $R^1 = Me$, $R^2 = Me$

- 7 $R^1 = H$, $R^2 = H$
 8 $R^1 = OEt$, $R^2 = OEt$
 9 $R^1 = SEt$, $R^2 = H$
 10 $R^1 = vinyl$, $R^2 = H$
 11 $R^1 = Et$, $R^2 = H$
 12 $R^1 = trans-propenyl$, $R^2 = H$

- 13 $R = H$
 14 $R = Me$

- 15 $R = H$
 16 $R = Me$

Table 1. Results of purified-enzyme COX-1 and COX-2 assays of compounds 1 to 16.

Compound	COX-1 IC_{50}^a (μM)	COX-2 IC_{50}^a (μM)	COX-1/COX-2 ^b
1	0.011 ± 0.001 (13)	0.010 ± 0.001 (14)	1.1
2	0.014 ± 0.004 (2)	0.014 ± 0.003 (4)	1.0
3	15 ± 5 (2)	>100 (3)	<0.15
4	7.7 ± 1.8 (13)	0.10 ± 0.01 (14)	77
5	0.063 ± 0.001 (2)	0.07 ± 0.02 (4)	0.9
6	15 ± 4 (3)	19 ± 6 (5)	0.79
7	0.010 ± 0.001 (2)	0.021 ± 0.001 (4)	0.48
8	25 ± 5 (2)	0.32 ± 0.09 (5)	78
9	3.1 ± 0.8 (2)	0.33 ± 0.09 (3)	9.4
10	1.3 ± 0.3 (3)	0.73 ± 0.20 (3)	1.8
11	5.8 ± 1.1 (2)	2.4 ± 0.9 (3)	2.4
12	1.4 ± 0.3 (3)	0.15 ± 0.05 (3)	9.3
13	0.19 ± 0.02 (2)	0.19 ± 0.10 (3)	1.0
14	15.5 ± 0.6 (2)	0.67 ± 0.10 (4)	23
15	0.10 ± 0.02 (2)	0.19 ± 0.04 (3)	0.53
16	10.5 ± 3.0 (4)	0.23 ± 0.09 (5)	45
DuP-697	4.6 ± 2.2 (2)	0.19 ± 0.01 (2)	24
NS-398	37 ± 4 (2)	0.09 ± 0.001 (2)	410

^a IC_{50} s from COX-1 and COX-2 purified enzyme assays⁹, performed in the presence of 100 μM arachidonic acid and 2 mM genapol. Each table entry gives the mean \pm standard error for the number of determinations given in parentheses. ^b Ratio of COX-1 and COX-2 IC_{50} s.

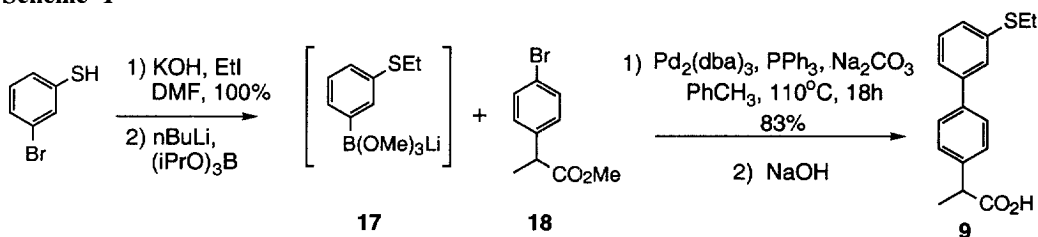
This could be interpreted as the result of steric differences or as a lack of good hydrogen bonding to the side channel. Comparing 2, 8, and 9, it appeared that the 3',5'-bisubstitution was important only if oxygen was the first atom in the 3' substituent. The greater COX-2 potency of the 3'-vinyl substituted 10 relative to the 3'-ethyl analog 11 verified the hypothesis that a planar conformation of the substituent with ring A (energetically favorable for 10 but not for 11) was important to properly occupy the alcove. *trans*-Methyl substitution of the double bond to go from a two-atom to a three-atom substituent in 12 introduced COX-2 selectivity as it did in previous cases. An alternative approach to dealing with the side channel was to replace the ring A phenyl with

a 3'-pyridine, which oriented the nitrogen lone pair towards the channel. Again, the 5'-vinyl analog **13** was potent but nonselective, while the *trans*-propenyl analog **14** was COX-2 selective (23-fold in this case).

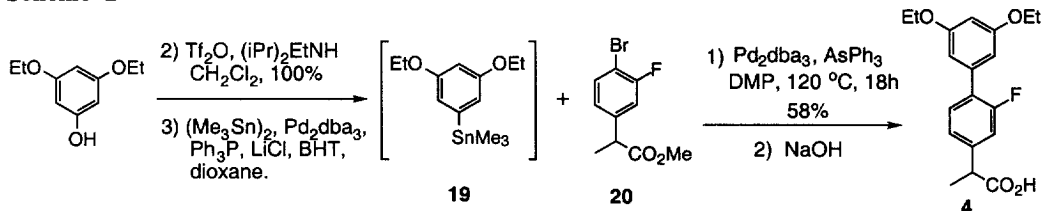
The aromatic ring of Tyr385, forming the ceiling of the alcove, was oriented so as to allow enough space for a five membered ring joining the 4' position to the 3' substituent (Figure 1a). Replacing ring A with an indole to make **15** would additionally allow a hydrogen bond to the Tyr385 aromatic ring in the spirit of a cation- π interaction.¹² The indole would only fit in on the "alcove" side; rotating it around to lie in the side channel is not allowed because of the tilted orientation of the Tyr385 ring (c.f. Figure 1). However, as far as the alcove itself is concerned, the simple indole would only occupy the equivalent of a two-atom chain; the methyl-substituted indole **16** would be required to occupy the alcove equivalent to a 3-atom linear 3' substituent. Compounds **15** and **16** were synthesized and assayed, **15** was potent but nonselective while **16** retained the COX-2 potency and gave 45-fold selectivity over COX-1.

Conclusion: This work demonstrates the use of structural information derived from X-ray crystal structures to rationally design COX-2 selectivity into the nonselective lead compound flurbiprofen. The initial binding mode of the flurbiprofen in COX-2 was predicted to bind in a manner similar to COX-1, which has been subsequently confirmed by an X-ray crystal structure.⁵ Optimal selectivity was conferred by a 3-atom lipophilic substituent in the 3' position of ring A, with an additional requirement of planarity with ring A. Systematic testing of the design hypothesis with regards to the requirements of the Leu384 alcove supported the hypothesis. With the ethoxy substituents, an unforeseen alternative binding mode of the ethoxy in the side channel introduced an additional requirement for 3',5'-bis-substitution before COX-2 selectivity was achieved. Three of these compounds, **4**, **8**, and **16**, show greater selectivity in our assay compared to the standard COX-2 selective compound DuP-697, though falling short of that of NS-398.

Scheme 1



Scheme 2



Synthesis: The compounds described in Table 1 were prepared by biaryl coupling methods as exemplified in Schemes 1 and 2. The majority of the compounds were synthesized using palladium-catalyzed Suzuki couplings of either aryl bromide **18**¹³ or the fluorinated aryl bromide **20**. The boronic acids were prepared from

commercially available aryl bromides in two or three step sequences using known chemistry. As illustrated for compound **9** in Scheme 1, this involved ethylation of 3-bromothiophenol with ethyl iodide followed by lithium-bromine exchange and trapping with triisopropyl borate. The crude lithium boronate was isolated by evaporating several times from methanol and was used directly in the coupling with **18**. Suzuki couplings were run in refluxing toluene with aqueous sodium carbonate in the presence of $\text{Pd}(\text{PPh}_3)_4$ freshly prepared from the $\text{Pd}_2(\text{dba})_3$ complex. For compounds **3** and **4**, the availability of phenols with the desired substitution pattern prompted us to pursue a Stille coupling strategy as illustrated for compound **4** in Scheme 2. Thus the readily prepared triflate was coupled with hexamethylditin to prepare the aryl stannane. This material was used without purification, and coupled with bromide **20** in DMF in the presence of $\text{Pd}(\text{AsPh}_3)_4$.¹⁴

References

1. Vane, J. R.; Botting, R. M. *Inflamm. Res.* **1995**, *44*, 1.
2. Smith, W. L.; Garavito, R. M.; DeWitt, D. L. *J. Biol. Chem.* **1996**, *271*, 33157.
3. Picot, D.; Loll, P. J.; Garavito, R. M. *Nature* **1994**, *367*, 243.
4. McKeever, B. M.; Pandya, S.; Percival, M. D.; Ouellet, M.; Bayly, C.; O'Neill, G. P.; Bastien, L.; Kennedy, B. P.; Adam, M.; Cromlish, W.; Roy, P.; Black, W. C.; Guay, D.; LeBlanc, Y., submitted for publication. Coordinates have been submitted to the Brookhaven Protein Databank with accession number 2CX2.
5. Luong, C.; Miller, A.; Barnett, J.; Chow, J.; Ramesha, C.; Browner, M. F. *Nature Struc Biol.* **1996**, *3*, 927.
6. Kurumbail, R. G.; Stevens, A. M.; Gierse, J. K.; McDonald, J. J.; Stegeman, R. A.; Pak, J. Y.; Gildehaus D.; Miyashiro, J. M.; Penning T. D.; Seibert, K.; Isakson, P. C.; Stallings, W. C. *Nature* **1996**, *384*, 644.
7. Gans, K. R.; Galbraith, W.; Roman, R. J.; Haber, S. B.; Kerr, J. S.; Schmidt, W. K.; Smith, C.; Hewes, W. E.; Ackerman, N. R. *J. Pharmacol. Exp. Ther.* **1990**, *254*, 180.
8. Futaki, N.; Yoshikawa, K.; Hamasaka, Y.; Arai, I.; Higuchi, S.; Iizuka, H.; Otomo, S. *Gen. Pharmacol.* **1993**, *24*, 105.
9. Copeland, R. A.; Williams, J. M.; Giannaras, J.; Nurnberg, S.; Covington, M.; Pinto D.; Pick, S.; Trzaskos, J. M. *Proc. Natl. Acad. Sci. U.S.A.* **1994**, *91*, 11202.
10. Ouellet, M.; Percival, M. D. *Biochem. J.* **1995**, *306*, 247.
11. Molecular dynamics simulations were carried out using AMBER 4.1: Pearlman, D. A., Case, D. A., Caldwell, J. W., Ross, W. S., Cheatham, T. E., Ferguson, D. M., Seibel, G. L., Singh, U. C., Weiner, P. J., Kollman, P. A., AMBER 4.1, University of California, San Francisco, 1995.
12. Ma, J. C.; Dougherty, D. A. *Chem. Rev.* **1997**, *97*, 1303.
13. (a) Yamauchi, T.; Nakao, K.; Fujii, K. *J. Chem. Soc. Perkin Trans. I* **1987**, 1433. (b) Yamauchi, T.; Hattori, K.; Nakao, K.; Tamaki, K. *J. Org. Chem.* **1988**, *53*, 4858. (c) Fujii, K.; Nakao, K.; Yamauchi, T. *Synthesis* **1982**, 456.
14. Farina, V.; and Roth, G. P. *Tetrahedron Lett.* **1991**, 4243–4246.